

Dear Author

Please use this PDF proof to check the layout of your article. If you would like any changes to be made to the layout, you can leave instructions in the online proofing interface. Making your changes directly in the online proofing interface is the quickest, easiest way to correct and submit your proof. Please note that changes made to the article in the online proofing interface will be added to the article before publication, but are not reflected in this PDF proof.

If you would prefer to submit your corrections by annotating the PDF proof, please download and submit an annotatable PDF proof by clicking [here](#) and you'll be redirected to our PDF Proofing system.



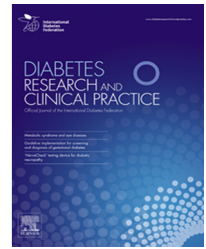
Contents available at ScienceDirect

Diabetes Research
and Clinical Practice

journal homepage: www.elsevier.com/locate/diabres



International
Diabetes
Federation



Study of the diacylglycerol composition in the liver and serum of mice with prediabetes and diabetes using MeV TOF-SIMS

Marijana Popović Hadžija^{a,*}, Zdravko Siketić^b, Mirko Hadžija^a, Marko Barac^b, Iva Bogdanović Radović^b

^a Division of Molecular Medicine, Laboratory for Mitochondrial Bioenergetics and Diabetes, Ruđer Bošković Institute, Bijenička cesta 54, 10000 Zagreb, Croatia

^b Division of Experimental Physics, Laboratory for Ion Beam Interactions, Ruđer Bošković Institute, Bijenička cesta 54, 10000 Zagreb, Croatia

ARTICLE INFO

Article history:

Received 4 September 2019

Received in revised form

15 November 2019

Accepted 17 December 2019

Available online xxxx

Keywords:

Lipids

Liver

Serum

Diabetes

MeV TOF-SIMS

ABSTRACT

Aims: Hepatic insulin resistance, induced by fat, occurs before peripheral resistance and leads to prediabetes and diabetes. If insulin resistance is detected earlier, lifestyle changes could prevent or delay disease development. Therefore, we analysed lipids in the liver and serum of prediabetic and diabetic mice by MeV TOF-SIMS with a focus on diacylglycerols (DAGs) as the best predictor of (liver) resistance.

Methods: Glucose impairment was spontaneously developed or induced by HFD in NOD/LtJ mice, and prediabetic and diabetic mice were selected according to their glucose levels. MeV TOF-SIMS was applied to image the lipid distribution in the liver and to relatively quantify lipids related to insulin resistance in both the liver and serum.

Results: The same lipids were detected in the liver and serum but with different intensities between mice. The intensity of DAGs and fatty acids was higher in the diabetic than that in the prediabetic liver.

Imaging of liver tissue showed a more compact density of prediabetic (non-fatty) than diabetic liver with DAG remodelling in diabetes. DAGs, which are greatly increased in diabetic serum, were successfully detected and quantified already in prediabetes.

Conclusion: MeV TOF-SIMS applied to the serum presents an excellent tool for *in vivo* monitoring of disease development over time.

© 2019 Published by Elsevier B.V.

1. Introduction

Our modern lifestyle and mechanized society often include physical inactivity accompanied by the consumption of a

high-calorie diet [1]. The consequence is energy imbalance, where caloric intake exceeds expenditure, thus contributing to the current epidemic of obesity.

Abbreviations: MeV TOF-SIMS, Time-of-Flight Secondary Ion Mass Spectrometry using MeV ions; HFD, high-fat diet; SFD, standard-fat diet; STIM, Scanning Transmission Ion Microscopy; DAGs, diacylglycerols; FAs, fatty acids; PC, phosphocholine

* Corresponding author at: Laboratory for Mitochondrial Bioenergetics and Diabetes, Division of Molecular Medicine, Ruđer Bošković Institute, Bijenička cesta 54, 10000 Zagreb, Croatia.

E-mail address: mhadzija@irb.hr (M. Popović Hadžija).

<https://doi.org/10.1016/j.diabres.2019.107986>

0168-8227/© 2019 Published by Elsevier B.V.

The liver is the major site for converting excess dietary carbohydrates and fats into fatty acids (FAs) and triglycerides, which are then deposited first in liver cells and later in adipose tissue. It is normal to have a small amount of fat in the liver, but the build-up of fat in the liver is connected with specific hepatic insulin resistance, metabolic syndrome, and prediabetes, which increases the risk for developing type 2 diabetes [2].

Experiments with high-fat diet (HFD)-fed rodent models have shown that consuming a HFD contributes to the chronic increase in circulating free FAs. A high rate of FAs is delivered into the liver through the liver-specific fatty acid transport protein 5 (FATP5), resulting in increased levels of long-chain fatty acids (LCoAs) [3,4], which can be converted to diacylglycerols (DAGs). DAG is a glyceride consisting of two fatty acid chains covalently bonded to a glycerol molecule through ester linkages, thus forming 1,2-diacylglycerols and 1,3-diacylglycerols. Therefore, saturated fatty acids are usually bonded at the C1 position and unsaturated fatty acids at the C2 or C3 position. The accumulation of DAGs containing saturated FAs in various intracellular compartments such as the membrane or lipid droplets in hepatocytes may interfere with β -cell function and insulin signalling, causing liver-specific insulin resistance [5–7].

The link between intrahepatic DAG accumulation and hepatic insulin resistance could be attributed to the activation of protein kinase C ϵ (PKC ϵ), which is the predominant PKC isoform activated in the liver with a much greater affinity for DAGs [8,9]. Lipid-induced enzyme activation inhibits insulin receptor substrate-2 (IRS-2) tyrosine phosphorylation by the insulin receptor kinase, leading to the inability of insulin to activate hepatic glycogen synthesis and the inability to suppress hepatic glucose production.

Intrahepatic fat vacuoles and hepatic insulin resistance in mice and rats can be induced with only 3 days of high-fat feeding before the development of obesity, muscle lipid accumulation or peripheral insulin resistance [8]. It has been demonstrated that ectopic lipids in the liver are specifically associated with hepatic insulin resistance. Among all correlated lipid components, Magkos et al. [10] demonstrated that the hepatic DAG content, but not hepatic ceramide content, was the best predictor of hepatic insulin resistance in obese humans. Additionally, shifts in lipids and lipoproteins at the periphery were detected early in the progression of metabolic syndrome in overweight rhesus monkeys, certainly by the time insulin resistance has developed and possibly even in advance of that [11]. Among them, the plasma diacylglycerol composition has been suggested as a biomarker of metabolic syndrome onset in rhesus monkeys [11].

After months or years of (hepatic) insulin resistance, blood sugar begins to rise, leading to prediabetes, when the glucose level is between 6.1 and 6.9 mmol/L (according to the WHO criteria for the diagnosis of prediabetes based on the fasting glucose level). In clinical settings, to check if someone has prediabetes, doctors commonly measure the fasting plasma glucose level and/or fasting blood glycosylated haemoglobin. At the same time, doctors do not test for insulin resistance since the hyperinsulinaemic-euglycemic clamp and intravenous glucose tolerance test, as the most reliable methods available for estimating insulin resistance, are time consum-

ing and expensive. If we can determine a marker of insulin resistance in the target tissues and/or in the serum earlier, it would be possible to make some immediate and lasting lifestyle changes that could help prevent not only the onset of type 2 diabetes but also all related complications, including heart disease, vision loss, nerve damage, and kidney failure. Taking into account all of the aforementioned factors, it is clear that determining DAGs in liver tissue and/or serum could play an important role in the prediction of early events in the development of gluco-regulatory impairment.

To our knowledge, there are several different ways to identify DAGs in biological samples. Most available kits use the competitive binding enzyme immunoassay system on microtitre plates. In that case, DAGs from the sample are captured on a pre-coated DAG-specific antibody and further visualized by applying enzyme-linked secondary antibody and substrate for producing visible signal, which is measured spectrophotometrically. The concentration of DAGs in the sample is determined by comparing the optical density of the samples to the standard curve.

Most of those kits are suitable for the analysis of cell lysate, plasma or serum, but some of them are able to measure the DAG content in tissue homogenate and collected supernatant, which can be applied on the microtitre plate.

DAGs in tissue can also be measured by thin layer chromatography (TLC) or liquid chromatography-mass spectrometry (LC-MS). For that purpose, tissue should be frozen and DAGs isolated through several steps that involve chloroform/methanol extraction, evaporation to dryness and redissolving in hexane-methylene chloride-ethyl ether and separation from triglycerides. The eluted DAG fraction is then evaporated to dryness and re-dissolved in solvent suitable for LC-MS analysis. Since the procedure for tissue preparation is complex and requires tissue homogenization, information about the 2D distribution of DAGs is lost.

It is obvious that all mentioned methods for measuring DAGs have some limitations, such as using species-specific primary antibodies, creating standard curves requirements for protocol optimization. To better understand the composition of biological samples as well as to evaluate chemical and structural pathological changes in the tissue, methods are required that offer detailed chemical information with high spatial distribution and sensitivity. The method that satisfies those conditions is Time-of-Flight-Secondary Ion Mass Spectrometry (TOF-SIMS).

TOF-SIMS was originally developed as a surface analysis technique for the identification and 2D molecular imaging of organic and inorganic materials by detecting secondary molecular ions released from the sample surface by a primary ion beam [12–14]. In recent years, the potential of the technique for implementation in life sciences has been widely explored. Fundamental advances, such as lateral resolution below 1 μ m and high sensitivity for the examination and characterization of lipids, allow the utilization of TOF-SIMS for studying lipid-related diseases [15,16]. Therefore it is possible to detect multiple lipid species directly from the sample surface, which is ideal for the analysis of complex biological systems under physiological or pathological conditions.

In recent years, the capability of TOF-SIMS for surface analysis and structural investigations in biological samples

has been greatly improved by using either cluster ion sources [17] or MeV ions for excitation, making identification of molecular species in the sample at the micron level easier.

We have already successfully applied MeV TOF-SIMS for imaging human adenocarcinoma cells at the subcellular level [18]. The goal of the present study was to determine early events in the development of glucoregulatory impairment in the prediabetic (spontaneously developed) and HFD-induced diabetic mouse model, with a focus on lipids in the liver tissue and also in the serum. In the liver, changes not only in the content of DAGs (as an insulin resistance predictor) but also in the content of FAs and cholesterol (whose increased levels are found in steatosis) have been determined. To our knowledge, this is the first application of MeV TOF-SIMS to determine the lipid content in mouse serum. The level of DAGs in the serum of prediabetic and diabetic mice correlates well with their blood glucose levels. Therefore, MeV TOF-SIMS is an excellent tool for tracing a lipid-based biomarker (DAGs) in the assessment of metabolic disruption and insulin resistance at an early phase, when it is possible to prevent or delay type 2 diabetes.

2. Materials and methods

2.1. Treatment of mice and preparation of mouse liver tissue and serum

To detect and measure compounds linked to hyperglycaemia/insulin resistance in complex biological samples (liver tissue and serum), the MeV TOF-SIMS method was applied. For that purpose, normoglycaemic NOD/LtJ mice (both sexes at 8 weeks of age) were fed with either SFD (11.4% fat, 4 mice) or HFD (58% fat, 4 mice) for 4 weeks. Both groups of mice were age-matched and housed in identical environments. For detection of hyperglycaemia, blood glucose levels were measured every week by glucometer in a blood drop taken from the tail vein. Before the measurement, mice were fasted for 6 h. All procedures were approved by the Ministry of Agriculture of Croatia, (No: UP/I-322-01/17-01/43 525-10/0255/17/3 from 19 May 2017) and carried out in accordance with associated guidelines of the EU Directive 2010/63/EU.

Two representative mice on different diets were selected for further MeV TOF-SIMS analysis according to their blood glucose levels in the last two measurements. The fasting glucose level in the blood of mouse on SFD was 6.3 mmol/L (fasting blood glucose level between 6.1 and 6.9 mmol/L is considered as prediabetes), but mouse on HFD was hyperglycaemic with a glucose concentration of 8.6 mmol/L (fasting blood glucose level equal to or higher than 7.0 mmol/L characterizes diabetes). Whole blood (20–30 μ l) taken from the tail vein was collected into the appropriate tube and allowed to form a clot. The clot was removed by centrifugation, and the resulting serum was pipetted in a clear vial and stored at -80°C until MeV TOF-SIMS measurements. The animals were sacrificed by cervical dislocation, and the liver was excised. In order to preserve liver morphology and the primary distribution of molecular species, a portion of the tissue was immediately embedded in Tissue-Tek OCT Compound for Cryostat Sectioning (Sakura, The Netherlands),

cryo-preserved in isopentane cooled with liquid nitrogen and stored at -80°C until cryo-sectioning and further analysis.

OCT-embedded blocks of frozen liver tissue were removed from the freezer and sectioned inside a cryostat-microtome held at -25°C . The liver tissue sections were selected to be 5 μm thick to allow transmission of 9 MeV O^{4+} ions through the sample to use high lateral resolution mode for MeV TOF-SIMS measurements [18]. One of the sections was immediately placed onto a 100-nm-thick Si_3N_4 window and freeze-dried overnight. The time for transferring the sample from the freeze-drying equipment to the vacuum chamber where MeV TOF-SIMS measurements were performed was kept below 30 min. Additional cryo-sections of mouse liver were stained by fat-soluble Sudan III dye for the visualization of intra-hepatic fat vacuoles.

In pilot experiments, the MeV TOF-SIMS measurement of the embedding OCT medium was performed in order to obtain the OCT molecular spectrum and to see if the mass peaks coming from the OCT interfere with the mass peaks relevant for the present measurements of liver tissue.

A portion of the mouse liver was fixed in 10% neutral buffered formalin, dehydrated in alcohol and cleared in xylene embedded in paraffin and cut into 5- μm -thick sections. Then, thin sections were stained with haematoxylin and eosin (H&E) according to the standard procedure [19]. Just before MeV TOF-SIMS analysis, serum samples were removed from -80°C . For each sample, a volume of 5 μl was dispersed as a thin film on a clean silicon wafer, dried for 2 min and immediately placed in the vacuum chamber for MeV TOF-SIMS measurements.

2.2. MeV TOF-SIMS analysis

Measurements were performed using a setup for MeV SIMS with linear TOF installed at the Ruđer Bošković Institute heavy ion microprobe. For homogeneous samples such as blood serum, only mass spectra were collected using the MeV TOF-SIMS setup with the pulsed ion beam. Since the used MeV TOF-SIMS spectrometer is linear type, without any timing focusing elements, mass resolution is $M/\Delta M \approx 400$ for $M = 262$ [20]. More details about the experimental setup can be found in Tadić et al. [20]. Focused 8 MeV Si^{4+} ions were scanned over an area of approximately $500 \times 500 \mu\text{m}^2$. The typical lateral beam resolution was approximately $8 \times 8 \mu\text{m}^2$.

In order to improve lateral resolution for imaging, a continuous beam was applied instead of the pulsed primary beam, allowing the start signal for TOF from the charge particle detector placed behind the thin transmission target. This detector is usually used for Scanning Transmission Ion Microscopy (STIM), a technique that is based on the energy loss of ions in the sample that can provide information about the sample density distribution. Therefore, together with molecular images, a STIM image of the sample density distribution was also recorded [26]. For the liver tissue measurements, 9 MeV O^{4+} ions were scanned over an area of approximately $360 \times 360 \mu\text{m}^2$, and the typical lateral beam resolution was approximately $1 \times 1 \mu\text{m}^2$. As shown in Stoytschev et al. [21], secondary molecular ion yields are, among other parameters,

directly proportional to the electronic stopping power of the primary ions used in the organic material, and therefore, for the sensitivity, it would be better to use silicon ions instead of oxygen as we have used for serum measurements. However, as ions have to be sufficiently energetic to reach the STIM detector after passing through the 5- μm -thick liver tissue sample, 9 MeV O^{4+} ions were selected.

Mass spectra and 2D images from liver tissue were collected using the in-house developed data acquisition system SPECTOR [22]. Positive and negative secondary molecular ions were extracted from the sample surface through the ± 4 kV potential difference toward the extractor and linear TOF. Data acquisition was controlled using SPECTOR software, while data processing and normalization were performed using the MATLAB software MSiReader [23] and mMass software [24]. All SIMS maps were normalised to the total number of counts, as is usually the case in TOF-SIMS imaging. Colour scale bars, with the amplitude representing the number of counts, are indicated to the right of each image.

3. Results and discussion

3.1. HFD-induced mouse model of fatty liver

Although the NOD strain of mice spontaneously develops an autoimmune type of diabetes, consuming a HFD leads to the faster development of impaired glucose tolerance and its complications (such as obesity and insulin resistance). The effect of high calorie intake could go directly through the promotion of beta-cell apoptosis [25,26] and indirectly through favoured lipid accumulation in hepatocytes, which has a dangerous effect on liver function, causing a high risk of developing liver insulin resistance [27,28].

In addition to the liver, muscles and fat can also become resistant to insulin with disease progression. The pancreas must produce more insulin to help glucose enter the cells due to insulin resistance in the target tissue. In people who already have some insulin resistance, prediabetes, the condition when blood glucose level is higher than normal (fasting blood glucose level between 6.1 and 6.9 mmol/L), usually occurs. If the pancreas could not make enough insulin to overcome a weak response to insulin, the blood glucose level will reach the diabetes diagnosis level (≥ 7.0 mmol/L). It is estimated that 25% of persons with prediabetes will fully develop diabetes over three to five years.

In order to prevent or delay the disease progression, recommendations to the people with prediabetes are to eat healthier and to lose some body weight.

It was already shown that specific lipids accumulated in the liver are associated with hepatic insulin resistance, which can be induced by a HFD [8]. Because resistance to insulin action in the liver is developed earlier than that in the periphery, it is very important to detect hepatic insulin resistance at the very beginning, when changes in the lifestyle or the appropriate therapy can be applied. Among hepatic lipids, the DAG content is the best predictor of liver insulin resistance [10].

As already mentioned, available methods for DAG detection involve complex protocols for sample preparation, and

none of the methods provide information about the spatial distribution of DAGs in tissues or cells. Here, we demonstrate that MeV TOF-SIMS can be used for the identification of not only DAGs (as a predictor of hepatic insulin resistance) but also cholesterol, phosphocholine (PC) and FAs, directly on the liver cryo-sections obtained from mice fed with a SFD or HFD. Since all these types of lipids are normally present in the liver, we were interested in observing changes in their levels (particularly the level of DAGs) after treatment of mice with HFD in which they already developed impaired glucose tolerance and hyperglycaemia.

This is important since the measurement of the 2D distribution across diseased tissue can reveal areas of abnormal chemistry, such as scarcity or over-abundance of a particular compound, thus connecting cellular dysfunction with anatomical specificity.

One of the characteristics associated with high calorie intake is body weight gain. NOD mice on a HFD were approximately 3 g heavier than mice on a SFD at the end of the experiment. According to the expectation, the average glucose value was higher (7.7 mmol/L) after consuming a HFD compared to the glucose level of mice fed with a SFD (6.0 mmol/L). Mice fed with a SFD or HFD that were selected for MeV TOF-SIMS analysis had fasting glucose levels of 6.3 mmol/L (prediabetes) and 8.6 mmol/L (diabetes), respectively, confirming that the HFD induced metabolic disturbance. First, we explored the grade of liver deterioration caused by treatment with HFD for 4 weeks. The staining of SFD and HFD liver paraffine-embedded or cryo-sections revealed that the tissue morphology was preserved (Fig. 1, upper and lower panels). In order to confirm the storage of fat in the vacuoles, standard Sudan III dye for the visualization of lipid droplets within the cytoplasm of hepatocytes was used for both mice. Fat vacuoles were predominately present in the liver of mouse fed with a HFD compared to the mouse fed a SFD (Fig. 1, lower panel). This confirms that our mouse model established by HFD is characterized by hyperglycaemia and also by fatty liver.

3.2. Imaging of liver tissue and measurement of biochemical composition

Since the sample preparation techniques, which should preserve the chemical and spatial integrity, are crucial for TOF-SIMS imaging, we have used the recommended technique for mouse liver preparation involving cryo-fixation in OCT medium, cryo-sectioning and freeze-drying [29].

The Scanning Transmission Ion Microscopy (STIM) imaging technique was first applied to assess the cryo-sections of 5- μm -thick liver tissue obtained from mice fed a SFD (Fig. 2a) or HFD (Fig. 2b). The area shown in the image is approximately $360 \times 360 \mu\text{m}^2$. On the left side of Fig. 2a, part of the Si_3N_4 frame can be seen where ions were completely stopped. The colour bar represents the density distribution from the highest (dark blue colour) to the lowest density (red colour). Black arrows indicate lipid vacuoles. From the figures, it can be concluded that the energy loss of 9 MeV O^{4+} ions is larger for the SFD (Fig. 2a) than that for the HFD (Fig. 2b), indicating that the tissue of the SFD liver is more

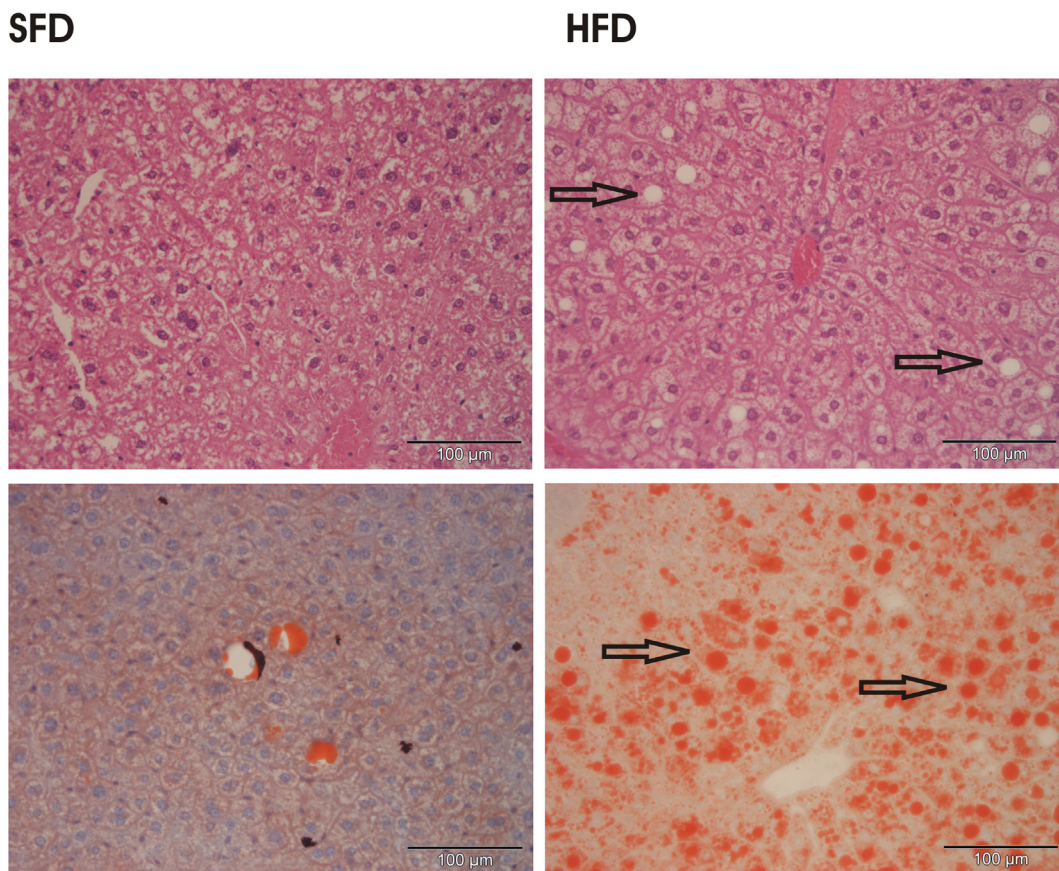


Fig. 1 – Liver sections of mice fed a standard-fat diet (SFD) and a high-fat diet (HFD) stained with H&E (upper panel) and with Sudan III (lower panel). The vacuoles and lipid droplets are marked with arrows.

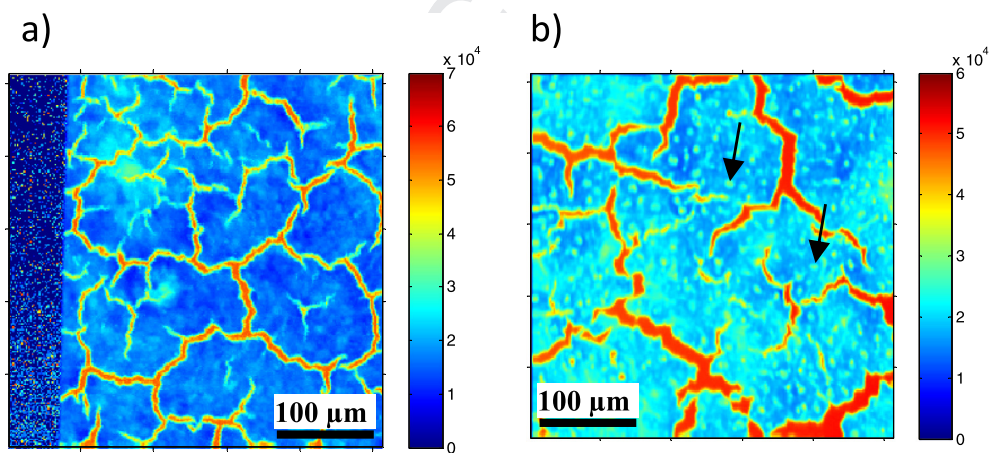


Fig. 2 – Scanning Transmission Ion Microscopy (STIM) image of 5- μm -thick liver tissue samples of mice fed with SFD (a) or HFD (b). The area of the image size is approximately $360 \times 360 \mu\text{m}^2$. The colour bar represents the density distribution from the highest (dark blue colour) to the lowest density (red colour). Black arrows indicate lipid vacuoles. From the figures, it can be concluded the energy loss of 9 MeV O^{4+} ions is larger for SFD (a) than for HFD (b) liver tissue, indicating that normal liver tissue is more dense than tissue with fat vacuoles. On the left side of (a), part of the Si_3N_4 frame can be seen where ions were completely stopped. (For interpretation of the references to colour in this figure legend, the reader is referred to the web version of this article.)

408 dense than that of the HFD liver. Moreover, the STIM image of
409 the HFD liver displays lipid vacuoles in the analysed area
410 (Fig. 2b, arrows), which are mostly absent in the image of

the liver from the mouse fed with SFD (Fig. 2a), which corre-
411 lates well with the numerous fat vacuoles detected by Sudan
412 III dye (Fig. 1, lower panel). Red colour presents regions with
413

414 lower energy loss, which morphologically might correspond
415 to the boundary between adjacent liver segments (Fig. 2).

416 The observed difference in the density of the liver tissue is
417 due to the changes in biochemical composition as a conse-
418 quence of consuming a high-fat diet, which is confirmed by
419 measuring mass spectra. As shown in Fig. 3a, the most pro-
420 nounced peaks in the spectra (measured in the positive ion
421 mode) belong to cholesterol (m/z 369.4), DAGs (DAG 32, m/z
422 552 and DAG 34, m/z 578) and PC (m/z 760). It should be
423 emphasized that the mass peaks of cholesterol and DAGs
424 from the mouse fed with the HFD (Fig. 3a, red) are much
425 higher than the same mass peaks belonging to the mouse
426 fed with the SFD (Fig. 3a, black). This correlates with the fatty
427 liver that developed in the mouse on a HFD, which was also
428 confirmed by Sudan III staining. Additionally, the FA mass

429 peaks (measured in the negative ion mode) are significantly
430 higher in the liver of HFD-fed mouse than in the liver of
431 SFD-fed mouse (Fig. 3b). Therefore, two groups of FAs were
432 identified: the first group FA16 (C16:1 (m/z 253.2) and C16:0
433 (m/z 255.2)) and the second group FA18 (C18:2 (m/z 279.2),
434 C18:1 (m/z 281.2) and C18:0 (283.2)). It is assumed that FA ions
435 are primarily part of TAGs and phospholipids [2].

436 As the specific role of DAGs in hepatic insulin resistance
437 [28,30] has already been explained, we further assessed the
438 composition and spatial distribution of DAG32 and DAG34
439 from mice fed with a SFD and HFD on the same liver sections
440 displayed in Fig. 2. The images recorded in the positive ion
441 mode show a homogenous distribution of DAGs throughout
442 the entire SFD liver section (Fig. 3c, upper panel), while in
443 the HFD liver, not only a higher number of accounts but also
444

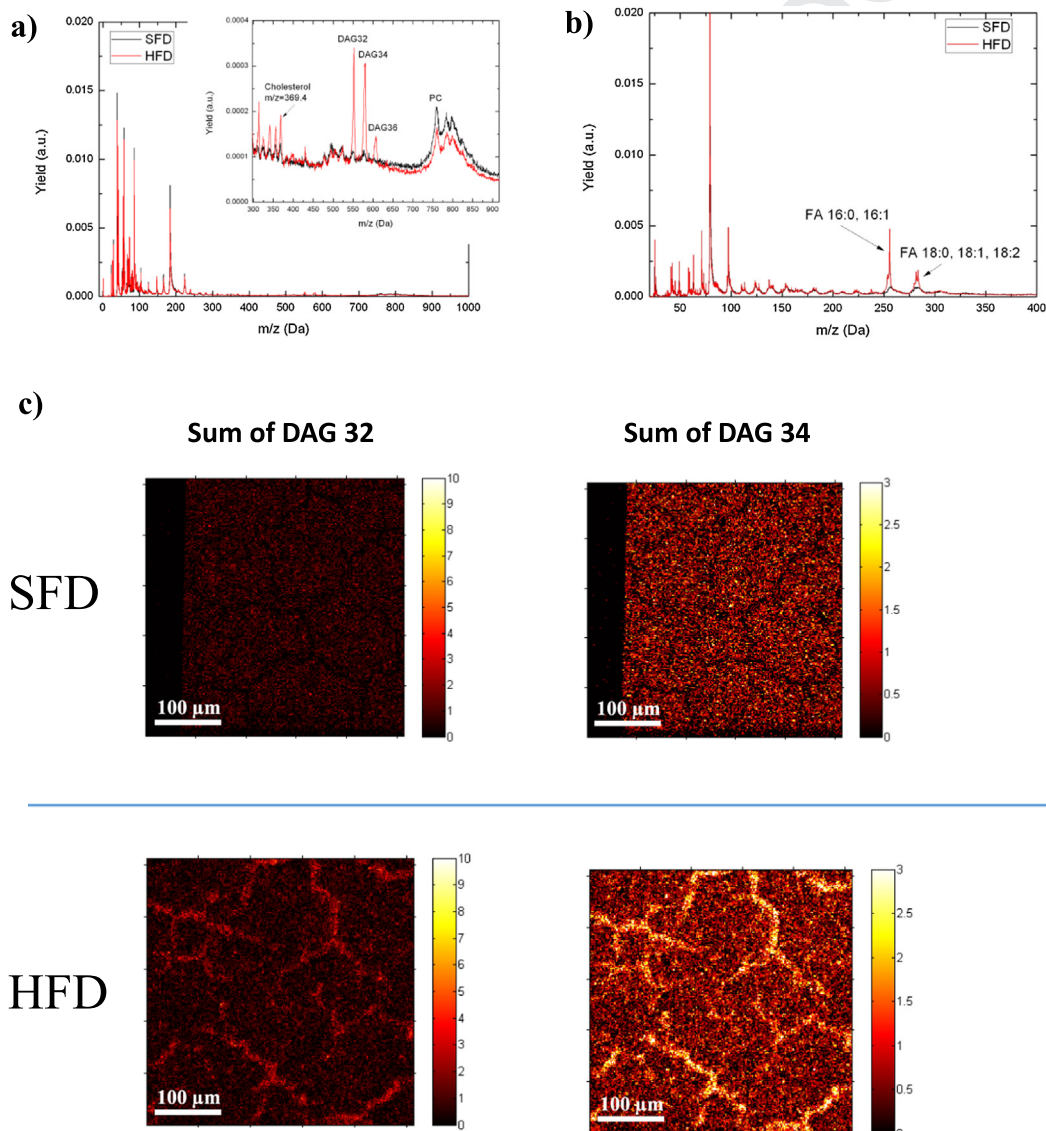


Fig. 3 – Mass spectra in positive (a) and negative (b) ion mode collected from liver cryo-sections of mice fed with SFD (black) or HFD (red). The peaks belonging to cholesterol, DAGs, PC and FAs are marked in the mass spectra. The spatial distribution (c) of DAG 32, m/z = 552 and DAG 34, m/z = 578 in the liver obtained from mouse on SFD (upper panel) or HFD (lower panel). Data are collected from the same tissue area shown in Fig. 2. (For interpretation of the references to colour in this figure legend, the reader is referred to the web version of this article.)

444 the spatial remodelling of DAGs (Fig. 3c, lower panel) was
445 observed. DAGs are dispersed over the analysed area, but
446 the largest amount is localized at the boundary of segments.

447 As can be concluded from Fig. 3a, some small amount of
448 DAGs exists already in SFD-fed mouse but peaks for DAG32,
449 DAG34 and DAG36 are significantly more pronounced in the
450 liver of HFD-fed mouse most likely due to the high calorie
451 intake or fragmentation of TAGs [31]. Cholesterol, as a mem-
452 brane lipid and mass spectrometric-friendly lipid molecule,
453 displayed a higher signal in fatty liver than in non-fatty liver
454 as a consequence of the disproportionate of caloric intake rel-
455 ative to expenditure. Some lipids are not detected *in situ*, such
456 as fatty acids with 20 carbon atoms, which might be either
457 due to the poor desorption/ionization yields or to intense
458 fragmentation of these compounds [30].

459 We can summarize that the same lipid classes are present
460 in the liver samples of both mice but with variations in their
461 relative intensities; DAGs and FAs showed a higher intensity
462 in the diabetic mouse with a fatty liver compared to the
463 mouse with non-fatty liver. Our results are in agreement with
464 the TOF-SIMS results obtained on the tissue samples of peo-
465 ple suffering from non-alcoholic fatty liver disease
466 [15,32,33]. Additionally, the method is successfully applied
467 to image the location and to quantify a single compound or
468 even a set of compounds in diseases such as colon dysplasia,
469 osteoporosis, breast cancer or chronic obstructive pulmonary
470 disease [34–37]. To our knowledge, the only work in which
471 TOF-SIMS was used to identify the changes in the lipid com-
472 position within mouse tissue (skeletal muscle, liver and adi-
473 pose tissue) in response to the dietary intake of omega-3
474 fatty acids was published by Sjovald et al. [2]. However, there
475 is lack of data about the dietary-induced events in insulin-
476 targeted tissues that precede or cause the loss of glucose
477 homeostasis. Here, we have shown that disrupted glucose
478 homeostasis is due to the increase in DAGs and FAs in the
479 liver.

480 3.3. MeV TOF-SIMS spectra of serum

481 It is obvious that HFD-induced disease in mouse liver stems
482 from dysfunctional metabolic processes of lipids. The
483 changes in lipid metabolism, transport and storage occur
484 early in the progression of impaired glucose tolerance, cer-
485 tainly by the time of insulin resistance or possibly even before
486 it. As demonstrated above, it can be related to the increased
487 accumulation of DAGs and FAs in the mouse liver of HFD-
488 fed animals compared to the SFD-fed animals (Fig. 3a, b).
489 Studies by other authors [10,11] have shown that DAGs are
490 specifically responsible for liver insulin resistance and conse-
491 quently impaired glucose homeostasis. The increase in glu-
492 cose concentration could be detected in plasma at the very
493 beginning, in the state of prediabetes that presents an inter-
494 mediate state of hyperglycaemia. Therefore, it is very likely
495 that metabolic changes caused by the accumulation of lipids
496 in the liver in this state also have an effect on the periphery
497 through the different intensities of DAGs and/or FAs. In order
498 to test our assumption, we applied the MeV TOF-SIMS
499 method to analyse serum from the same SFD- and HFD-fed
500 mice from which liver samples were taken.

501 Only 5 μ l of serum was dispersed on a clean silicon wafer
502 as a fine, thin film and dried only a few minutes before the
503 MeV TOF-SIMS measurement. As shown in Fig. 4a, b, serum
504 samples produce very clear mass spectra in positive and neg-
505 ative mode, with the most pronounced peaks from choles-
506 terol, DAGs, PC and FAs. Among all those peaks, only peaks
507 belonging to DAGs are greatly increased in the serum of
508 HFD-fed mouse compared to the serum of mouse fed with
509 SFD. This is consistent with results from the liver tissue,
510 where higher levels of DAGs in HFD- than in SFD-fed mouse
511 were measured. This is in agreement with the observations
512 of other researchers found in the literature [10,11] that the
513 DAG composition could be taken as an early plasma marker
514 for assessment of a metabolic syndrome risk or a marker of
515 liver resistance.

516 It should be noted that the levels of FAs and cholesterol in
517 the serum of HFD- and SFD-fed mice are almost equal,
518 although simultaneously the same compounds in the liver
519 are present at slightly higher levels in the HFD- than in the
520 SFD-fed mouse (comparison of Figs. 3 and 4). From that, it
521 can be concluded that the level of cholesterol and FAs in the
522 mouse liver is below a critical capacity of accumulation to
523 affect the periphery. The increase in both components with
524 diabetes development (increasing hyperglycaemia), could be
525 expected, but this should be investigated in the future. As
526 far as the authors know, the MeV TOF-SIMS method was
527 applied for the first time to analyse serum, and even a small
528 volume (5 μ l) was more than sufficient to perform the analy-
529 sis. It should be emphasized that in the serum, mass spec-
530 trum peaks belonging to several lipid species could be
531 clearly seen as well as the differences in the relative peak
532 intensities.

533 4. Conclusions

534 The goal of this preliminary study was to determine events in
535 the spontaneously developed or HFD-induced impairment of
536 glucose homeostasis (state of prediabetes and diabetes), with
537 a focus on lipids in the target tissue (liver) and body fluid
538 (serum). The MeV TOF-SIMS method was applied to image
539 the distribution of lipids in liver cryo-sections and to quantify
540 the relative amount of lipid species related to insulin resis-
541 tance/hyperglycaemia (particularly DAGs) in both liver and
542 serum. The most pronounced peaks were peaks belonging
543 to DAGs, FAs, cholesterol and PC. However, the peak intensi-
544 ties varied between the prediabetic and diabetic mouse and
545 between the type of sample (liver vs serum). DAGs and FAs
546 showed a higher intensity in the liver of diabetic mouse with
547 a fatty liver compared to the prediabetic mouse with a non-
548 fatty liver. Moreover, we observed the spatial remodelling of
549 DAGs in the diabetic liver. The image of the density distribu-
550 tion showed a more compact density of prediabetic (non-
551 fatty) liver than diabetic liver (fatty liver) due to accumulated
552 fat in hepatocytes.

553 Among all peaks detected in serum, only peaks of DAGs
554 were significantly increased in the serum of diabetic mouse.
555 However, it should be emphasized that the DAG level was suc-
556 cessfully detected already in the periphery of prediabetic

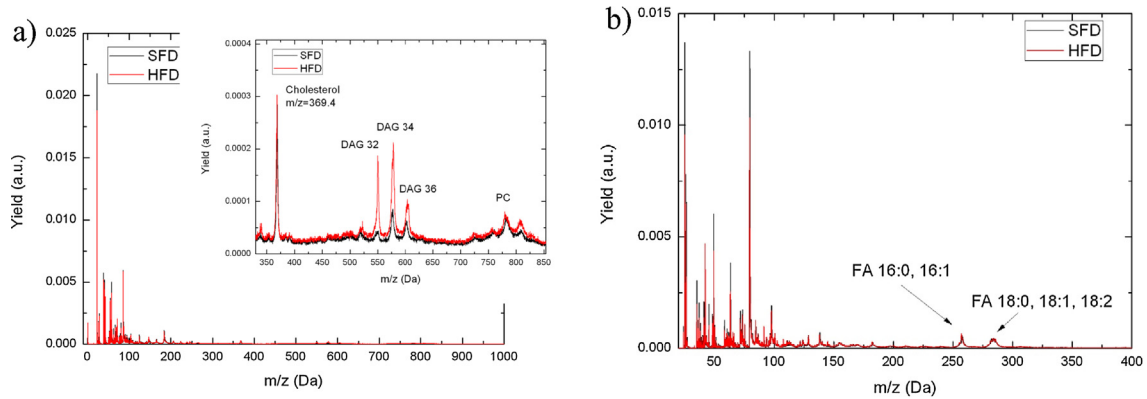


Fig. 4 – Mass spectra collected in the positive (a) and negative (b) ion mode of serum obtained from mice fed with SFD (black) and HFD (red). The peaks belonging to cholesterol, DAGs, PC and FAs are marked. (For interpretation of the references to colour in this figure legend, the reader is referred to the web version of this article.)

557 mouse, and it could be compared to the level found in the
558 serum of diabetic mouse.

559 Increased amounts of DAGs in the serum might be a dis-
560 tinctive marker providing information about increased accu-
561 mulation of lipids in the liver (confirmed by Sudan III dye in
562 our animal model) and the development of liver insulin resis-
563 tance. These results clearly demonstrate that serum (not only
564 specific tissues) can be useful for studying metabolic changes,
565 and the combination of the MeV TOF-SIMS method and
566 serum presents an excellent tool for *in vivo* investigation
567 because serum is much easier to prepare than tissue samples,
568 and a very small amount of serum is sufficient for the analy-
569 sis. An animal does not have to be sacrificed, and samples can
570 be taken from the same animal, allowing monitoring of dis-
571 ease development over time, which will be the subject of
572 our future work.

573 Although the MeV TOF-SIMS method cannot acquire abso-
574 lute quantitative data, the relative quantification comparing
575 mass spectra of healthy and pathological samples is possible.
576 The method is highly informative because the detected com-
577 pounds have a high biological significance, providing new
578 insights into the understanding of hepatic lipid metabolism
579 in normal and diabetic conditions.

580 Declaration of Competing Interest

581 The authors declare that they have no known competing
582 financial interests or personal relationships that could have
583 appeared to influence the work reported in this paper.

584 Acknowledgement

585 The authors thank Ms. Marina Marš for the excellent techni-
586 cal assistance. This work is supported through grant IP-2016-
587 06-1698 “Development of the capillary microprobe MeV SIMS
588 with the application on analysis of biological samples”
589 funded by the Croatian Science Foundation (Hrvatska Zaklada
590 za Znanost) and European Regional Development Fund for the
591 “Centre of Excellence for Advanced Materials and Sensing
592 Devices” (Grant No. KK.01.1.1.01.0001).

Author contributions

M.P.H., established animal model, performed biomedical
research, wrote the paper.

Z.S., designed research by MeV TOF-SIMS, performed MeV
TOF-SIMS analysis, wrote the paper.

M.B., collected and analysed the MeV TOF-SIMS data.

M. H., interpreted the data relevant to the animal model.

I. B. R., the principal investigator of the project, wrote the
paper.

REFERENCES

- [1] Lai M, Chandrasekera C, Barnard DN. You are what you eat, or are you? The challenges of translating high-fat-fed rodents to human obesity and diabetes. *Nutr Diab* 2014;4:e135.
- [2] Sjöval P, Rossmeisl M, Hanrieder J, Kuda O, Kopecky J, Bryhn M. Dietary uptake of omega-3 fatty acids in mouse tissue studied by time-of-flight secondary ion mass spectrometry (TOF-SIMS). *Anal Bioanal Chem* 2015;407:5101–11.
- [3] Schaffer JE, Lodish HF. Expression cloning and characterization of a novel adipocyte long chain fatty acid transport protein. *Cell* 1994;79:9427–36.
- [4] Shulman GI. Cellular mechanisms of insulin resistance. *J Clin Invest* 2000;2000(106):171–217.
- [5] Kahn SE, Hull RL, Utzschneider KM. Mechanisms linking obesity to insulin resistance and type 2 diabetes. *Nature* 2006;14:840–6.
- [6] Cantleya JLT, Yoshimurab JPG, Camporezb D, Zhanga FR, Jornayvazb N, Kumashiroa F, et al. CGI-58 knockdown sequesters diacylglycerols in lipid droplets/ER-preventing diacylglycerol-mediated hepatic insulin resistance. *PNAS* 2013;110:1871–7.
- [7] Finck BN, Hall AM. Does diacylglycerol accumulation in fatty liver disease cause hepatic insulin resistance? *Bio Med Res International* 2015;104:132–8.
- [8] Samue VT, Liu ZX, Qu X, Elder BD, Bilz S, Befroy D, et al. Mechanism of hepatic insulin resistance in non-alcoholic fatty liver disease. *J Biol Chem* 2004;279:32345–53.
- [9] Dries DR, Gallegos LL, Newton AC. A single residue in the C1 domain sensitizes novel protein kinase C isoforms to cellular diacylglycerol production. *J Biol Chem* 2007;282:826–30.

- 632 [10] Magkos X, Fabbrini E, Conte C, Eagon JC, Varela JE, Brunt EM, 683
633 et al. Intrahepatic diacylglycerol content is associated with 684
634 hepatic insulin resistance in obese subjects. 685
635 *Gastroenterology* 2012;2012(142):1444–5. 686
- 636 [11] Polewski MA, Burhans MS, Zhao M, Colman RJ, 687
637 Shanmuganayagam D, Lindstrom MJ, et al. Plasma 688
638 diacylglycerol composition is a biomarker of metabolic 689
639 syndrome onset in rhesus monkeys. *J Lipid Res* 690
640 2015;56:1461–70. 691
- 641 [12] Touboul D, Laprevote O, Brunelle A. Micrometric molecular 692
642 histology of lipids by mass spectrometry imaging. *Curr Opin 693*
643 *Chem Biol* 2011;15:725–32. 694
- 644 [13] Touboul D, Halgand F, Brunelle A, Kersting R, Tallarek E, 695
645 Hagenhoff B, et al. Tissue molecular ion imaging by gold 696
646 cluster ion bombardment. *Anal Chem* 2004;76:1550–9. 697
- 647 [14] Borner KB, Malmberg P, Mansson JE, Nygren H. Molecular 698
648 imaging of lipids in cells and tissues. *Int J Mass Spectrom 699*
649 2007;260:128–36. 700
- 650 [15] Debois D, Bralet MP, Le Naour F, Brunelle A, Laprevote O. *In 701*
651 *Situ* lipidomic analysis of nonalcoholic fatty liver by cluster 702
652 TOF-SIMS imaging. *Anal Chem* 2009;81:2823–31. 703
- 653 [16] Malmberg P, Borner K, Chen Y, Friberg P, Hagenhoff B, 704
654 Mansson JE, et al. Localization of lipids in the aortic wall with 705
655 imaging TOF-SIMS. *Biochim Biophys Acta Mol Cell Biol Lipids 706*
656 2007;2007(1771):185–95. 707
- 657 [17] Fearn S. Characterisation of biological material with ToF- 708
658 SIMS: a review. *Mater Sci Technol* 2015;31:148–61. 709
- 659 [18] Siketić Z, Bogdanović Radović I, Jakšić M, Popović Hadžija M, 710
660 Hadžija M. Submicron mass spectrometry imaging of single 711
661 cells by combined use of mega electron volt time-of-flight 712
662 secondary ion mass spectrometry and scanning 713
663 transmission ion microscopy. *Appl Phys Lett* 714
664 2015;107:093702–93706. 715
- 665 [19] [https://www.protocolonline.com/histology/dyes-and- 716](https://www.protocolonline.com/histology/dyes-and-stains/haematoxylin-eosin-he-staining/)
666 [stains/haematoxylin-eosin-he-staining/](https://www.protocolonline.com/histology/dyes-and-stains/haematoxylin-eosin-he-staining/). 717
- 667 [20] Tadic T, Bogdanovic Radovic I, Siketic Z, Cosic DD, Skukan N, 718
668 Jaksic M, et al. Development of a TOF SIMS setup at the 719
669 Zagreb heavy ion microbeam facility. *Nucl Instrum Meth 720*
670 *Phys Res B* 2014;332:234–7. 721
- 671 [21] Stoytschew V, Bogdanović Radović I, Demarche J, Jakšić M, 722
672 Matjačić M, Siketić Z, et al. MeV-SIMS yield measurements 723
673 using a Si-PIN diode as a primary ion current counter. *Nucl 724*
674 *Instrum Meth* 2016;B371:194–8. 725
- 675 [22] Bogovac M, Bogdanović I, Fazinić S, Jakšić M, Kukec L, 726
676 Wilhelm W. Data acquisition and scan control system for 727
677 nuclear microprobe and other multiparameter experiments. 728
678 *Nucl Instrum Meth B* 1994;1994(89):219–22. 729
- 679 [23] Robichaud G, Garrard KP, Barry JA, Muddiman DC. Infrared 730
680 matrix-assisted laser desorption electrospray ionization (IR- 731
681 MALDESI) imaging source coupled to a FT-ICR mass 732
682 spectrometer. *J Am Soc Mass Spectrom* 2013;24:718–21. 733
- [24] Strohmalm M, Kavan D, Novák P, Volný M, Havlíček V. mMass 3: 683
684 a cross-platform software environment for precise analysis 685
686 of mass spectrometric data. *Anal Chem* 2010;82:4648–51. 687
- [25] Linn T, Strate C, Schneider K. Diet promotes beta-cell loss by 688
689 apoptosis in prediabetic nonobese diabetic mice. 690
691 *Endocrinology* 1999;140:3767–73. 692
- [26] Gannon M. High fat diet regulation of β -cell proliferation and 693
694 β -cell mass. *TOEJ* 2010;4(1):66–77. Available from: [http:// 695](http://benthamopen.com/ABSTRACT/TOEJ-4-66)
696 benthamopen.com/ABSTRACT/TOEJ-4-66. [https://doi.org/ 697](https://doi.org/10.2174/1874216501004010066)
698 [10.2174/1874216501004010066](https://doi.org/10.2174/1874216501004010066). 699
- [27] Weiss R, Dufour S, Taksali SE, Tambortlane WV, Petersen KF, 700
701 Bonadonna RC, et al. Prediabetes in obese youth: a syndrome 702
703 of impaired glucose tolerance, severe insulin resistance, and 704
705 altered myocellular and abdominal fat partitioning. *Lancet* 706
707 2003;2013(362):951–7. 708
- [28] Derek ME, Shulman GI. Diacylglycerol-mediated insulin 709
710 resistance. *Nat Med* 2010;16:400–2. 711
- [29] Passarelli MK, Winograd N. Lipid Imaging with Time-of-Flight 712
713 Secondary Ion Mass Spectrometry (ToF-SIMS). *Biochim 714*
715 *Biophys Acta* 2011;2011(1811):976–90. 716
- [30] Debois D, Bralet MP, Le Naour F, Brunelle A, Laprevote O. *In 717*
718 *situ* lipidomic analysis of nonalcoholic fatty liver by cluster 719
720 TOF-SIMS imaging. *Anal Chem* 2009;81:2823–31. 721
- [31] Malmberg P, Nygren H, Richter K, Chen Y, Dangard F, Friberg 722
723 PP, et al. Imaging of lipids in human adipose tissue by cluster 724
725 ion TOF-SIMS. *Microsc Res Tech* 2007;70:828–35. 726
- [32] Puri P, Baillie RA, WiestMM Mirshahi F, Choudhury J, Cheung 727
728 O, et al. A lipidomic analysis of nonalcoholic fatty liver 729
730 disease. *Hepatology* 2007;46:1081–90. 731
- [33] Araya J, Rodrigo R, Videla LA, Thielemann L, Orellana M, 732
733 Pettinelli P, Poniachik. Increase in long-chain 734
735 polyunsaturated fatty acid n - 6/n - 3 ratio in relation to 736
737 hepatic steatosis in patients with non-alcoholic fatty liver 738
739 disease. *J Clin Sci* 2004;106:635–43. 740
- [34] Urbini M, Petito V, de Notaristefani F, Scaldaferrri F, Gasbarrini 741
742 A, Tortora L. TOF-SIMS and principal component analysis of 743
744 lipids and amino acids from inflamed and dysplastic human 745
746 colonic mucosa. *Anal Bioanal Chem* 2017;409:6097–111. 747
- [35] Schaepe K, Werner J, Glenske K, Bartiges T, Henss A, Rohnke 748
749 M, et al. TOF-SIMS study of differentiation of human bone- 749
750 derived stromal cells: new insights into osteoporosis. *Anal 751*
752 *Bioanal Chem* 2017;409:4425–35. 753
- [36] Angerer TB, Magnusson Y, Landberg G, Fletcher JS. Lipid 754
755 heterogeneity resulting from fatty acid processing in the 756
757 human breast cancer microenvironment identified by GCIB- 758
759 TOF-SIMS imaging. *Anal Chem* 2016;88:11946–54. 760
- [37] Najafinobar N, Venkatesan S, von Sydow L, Klarqvist M, 761
762 Olsson H, Zhou XH. TOF-SIMS mediated analysis of human 763
764 lung tissue reveals increased iron deposition in COPD (GOLD 765
766 IV) patients. *Sci Rep* 2019;9. 767